



Numerical Investigation of Sinusoidal and Trapezoidal Piston Profiles for an IC Engine

S. Kaliappan^{1†}, S. Mohanamurugan² and P. K. Nagarajan³

¹ Department of Mechanical Engineering, Velammal Institute of Technology, Chennai-601204, India

² Department of Mechanical Engineering, Aarupadai Veedu Institute of Technology,
 Old Mahabalipuram Road, Chennai-603104, India

³ Department of Mechanical Engineering, S.A Engineering College, Chennai-602105, India

†Corresponding Author Email: kaliappa@yahoo.com

(Received November 30, 2018; accepted May 21, 2019)

ABSTRACT

This paper is aimed at a comparative investigation on two different velocity profiles for piston movement namely Sinusoidal and Trapezoidal Profiles for an IC Engine. In conventional IC Engine, velocity profile of piston motion is Sinusoidal. It has many disadvantages such as high mean velocity that leads to high inertial force, frictional losses, wear and high rate of heat leakages. Nearly 20% of the total power produced by the engine is dissipated into heat because of friction. Of this 20%, about 75% is due to friction of piston rings on the cylinder walls. This is an irreversible loss and can be seen as a consequence of high mean piston velocity associated with the existing Sinusoidal Piston Velocity Profile. In addition, varying velocity profile can cause rapid acceleration and finally jerks which lead to considerable mechanical vibration and noise. As a result the mechanical strength of engine material will be high to withstand the inertial force, friction and wear. To overcome these difficulties, an extensive attempt is made to improve the piston movement by restructuring the piston velocity profile with reduced mean velocity which is constant for most of the crank angle. A comprehensive experimental examination is conducted for the Sinusoidal velocity profile, which are utilized in arriving at an optimal CFD procedure through validation study. A proposed connecting rod configuration with internal gear and pinion arrangement is proposed to achieve different Trapezoidal Profiles. The optimum CFD procedure found from validation study is used to analyze and understand the engine with modified Trapezoidal Velocity Profiles. There is almost 20% reduction of mean piston velocity that considerably improves hydro-thermo dynamic and mechanical characteristics of the existing engine.

Keywords: CFD; Sinusoidal; Trapezoidal; Hydro-thermo dynamic and Mechanical characteristics.

NOMENCLATURE

a	radius of crank	S_i	source or sink term for energy
B	cylinder bore	S_{Mx}	source or sink term for momentum
D_b	bearing diameter	TI	turbulence intensity
IC Engine	Internal Combustion Engine	T_n	tumble ratio
I_s, I_t	the moment of inertia with respect to swirl axis and tumble axis respectively.	\vec{u}	flow velocity vector
\bar{J}_i	diffusion flux of species i	ω_s, ω_t	angular velocity of rotating flow at swirl axis and at tumble axis respectively
L	connecting rod length	θ	crank angle
L_s, L_t	the angular moment with respect to swirl axis and tumble axis respectively	Γ	diffusion coefficient
m	module	τ_r	relaxation time of the diesel droplet
Ri	the net rate of production of species i by chemical reaction	ρ_p	density of diesel particle

1. INTRODUCTION

Recently many significant improvements are introduced in the development of Internal Combustion Engines with the goals of maximizing the work and power output, minimizing irreversible entropy losses (Rubin, 1979), increasing proper air fuel mixing to create efficient combustion, emission control etc. Many geometrical modifications and process methodologies are being suggested to ascertain an efficient non-power and power strokes. With the development in computational methodology many algorithms are utilized to model the entire physics, analytically and numerically. Empirical and semi-empirical correlations are devised (Shyy, 1994) to know underlying hydro-thermo dynamic process which is highly transient with very less cycle time. Piston motion and its trajectory is one of the influencing parameters that control the complex physics during power and non-power strokes (Taylor, 1966). Though enormous literatures are available in optimizing the shape of the combustion chamber, inlets and outlet orientations, fuel injector configuration and positions but very little data is available on optimum piston trajectory. The optimal piston motions of adiabatic Internal Combustion Engines for the maximum efficiency, work output and minimum entropy generation was investigated (Teh *et al.*, 2006a, 2006b). An optimal piston trajectory for each stroke by devising an eccentric shaft design was found (Chen *et al.*, 2009, 2011). It was claimed by them that, optimizing the piston motion for the cases with unconstrained and constrained piston accelerations are derived on each stroke by applying optimal control theory. It shows that optimizing the piston motion for the case of radiative heat transfer law can improve both the network output per cycle and the net efficiency by more than 7%. Based on these references, this paper will investigate hydro-thermo and turbulence behavior of a four stroke Diesel Engine cycle for a modified Trapezoidal Piston Profile over an existing Sinusoidal Piston Profile. Over the past few decades Computational Fluid Dynamics (CFD) is comprehensively used in successful modeling of complex multiphase interaction, dynamic meshing, particle tracking, particle break up, finite chemical reactions etc. (Qi *et al.*, 2011; Nigus, 2015; Prasad *et al.*, 2011; Rakopoulos *et al.*, 2010).

Sinusoidal Profiles are prominent for the generation of proper flow dynamics that is required for efficient combustion. The level of turbulence intensity, swirl ratio, tumble ratio have been properly designed for this type of profile over a long period. The noteworthy disadvantages associated with this profile are high mean velocity that leads to high inertial force, frictional losses, wear, high rate of heat leakages, rapid acceleration and finally jerks, vibration and noise (De Vos 1985).

The Trapezoidal Profiles have advantage over the Sinusoidal Trajectory in the above said conditions. In this work a connecting rod configuration that has internal gear and pinion arrangement which

develops Trapezoidal Piston Movement is proposed. Different gear combinations with different module values are used to form the four distinct Trapezoidal Profiles. The different mathematical expressions for Trapezoidal Piston Trajectory by varying internal gear, pinion teeth values and module are found.

An extensive study, conducted using CFD is utilized to find the optimum Trapezoidal Profile from the four combinations that has the flow dynamics performances similar with that of the Sinusoidal Profile with the considerable reduction of losses.

To validate CFD procedure an experimental investigation is done for existing engine with Sinusoidal Piston Movement. The appropriate computational methodology is arrived from this validation study and applied to arrive the Optimum Trapezoidal Trajectory.

2. EXISTING SINUSOIDAL MOTION/MODIFIED MOTION PROFILE COMPARISON

For the conventional engine, the displacement and velocity of piston with respect to crank angle (θ) as

$$x = a((1 - \cos \theta) + \sin 2\theta / 2R) \quad (1)$$

$$v = a\omega(\sin \theta + \sin 2\theta / 2R) \quad (2)$$

Where x , v –Displacement and Velocity of Piston respectively, a - Radius of Crank, R -the ratio of Length of connecting rod to the Radius of Crank = L/a , L - Length of connecting rod (Nigus, 2015).

An expression for reciprocating friction loss was developed (Kamil *et al.*, 2014) as

$$\begin{aligned} FMEP_{\text{recip}} = & C_{ps} \sqrt{\frac{\mu}{\mu_0}} \left(\frac{\bar{S}_p}{B} \right) \\ & + C_{pr} \left(1 + \frac{500}{N} \right) \left(\frac{1}{B^2} \right) \\ & + 3.03 \times 10^{-4} \sqrt{\frac{\mu}{\mu_0}} \left(\frac{ND_b^3 L_b n_b}{B^2 L_{nc}} \right) \end{aligned} \quad (3)$$

Where Constant $C_{ps} = 294$ kPa-mm-s/m, μ is the Viscosity, μ_0 is the Reference Viscosity, \bar{S}_p is the Mean Piston Speed, Constant $C_{pr} = 4.06 \times 10^4$ KPa-mm², N is the Engine Speed, B is Cylinder Bore, D_b is the Bearing Diameter, L_b is the Bearing Length, n_b is the Number of Bearings, n_c is the Number of Cylinders.

This clearly indicates that frictional loss varies almost linearly with mean piston speed.

The Friction Mean Effective Pressure versus Crank Angle for both two concepts as shown in Fig. 1.

A modified piston velocity trajectory considering power and non-power stroke with the help of Hamiltonian expression was developed (Lingen Chen *et al.*, 2011, Badescu, 2004), where the goal

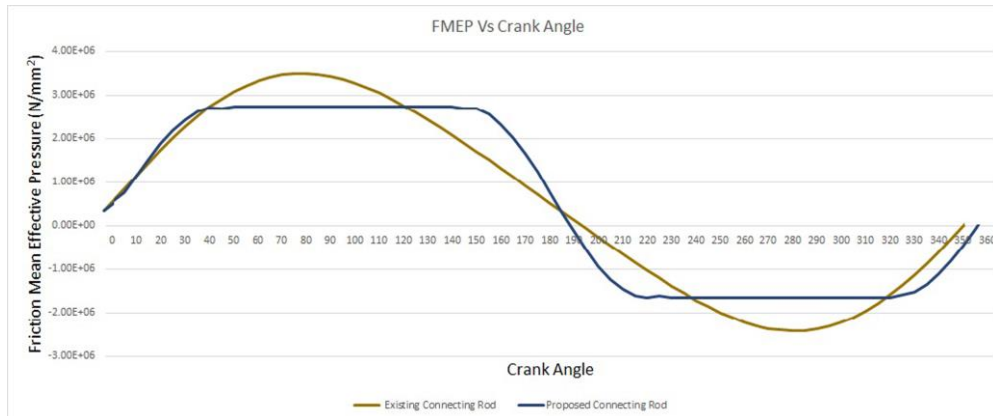


Fig. 1. FMEP Vs Crank Angle.

was to minimize the friction loss. The velocity profile versus time looks highly non-linear and an eccentric shaft mechanism is developed for producing such motion. Referring to his work another mechanism is introduced here which is relatively simple that keeps all the power and non-power stroke Trapezoidal.

A Proposed connecting rod has internal gear and pinion arrangement as shown in Fig. 2 (Kaliappan *et al.*, 2018).

A relation between stroke length and module is established and expressed as

$$\text{Stroke} = \text{Rack length} + \left(\frac{\text{No. of Teeth in Gear} - \text{No. of Teeth in Pinion}}{m} \right) \quad (4)$$

The piston position for different crank angles are calculated by using the Equations.

For 0° to 40° crank angle rotation (From TDC to BDC)

By using Law of Cosine formula,

$$\sqrt{(L + (13 + 5\pi)m + 4m \cos(2.25\theta))^2 + (4m \sin(2.25\theta))^2} \quad (5)$$

For next 100° crank angle rotation

By using Pythagoras theorem,

$$\sqrt{(L + (13 + 5\pi)m - 0.05\pi m (\theta - 40))^2 + (4m)^2} \quad (6)$$

For next 40° crank angle rotation

By using Law of Cosine formula,

$$\sqrt{(L + 13m - 4m \cos(2.25(180 - \theta)))^2 + (4m \sin(2.25(180 - \theta)))^2} \quad (7)$$

Where m-Module θ - Crank Angle, BDC- Bottom Dead Center, TDC- Top Dead Center.

The stroke is calculated from the piston position by calculating the maximum position of piston and current position of piston. From the Stroke the displacement and velocity values are calculated. For the remaining rotation of crank angle from 180° to 360° is taken as symmetrical. The velocity values represented as Trapezoidal Trajectory. The piston velocity profile is arrived for various combinations of pinion and gear teeth values (18-26, 18-28, 20-28

and 20-30) with different compression ratios (14, 17.5 and 21). From these combinations, the pinion and gear teeth (18-26) and compression ratio (17.5) is correlating with conventional connecting rod system.

The entire comparative study is conducted for constant compression ratio of 17.5 and constant speed of 1500 rpm. The Fig. 3 shows the comparison of velocity profile for Proposed and Conventional connecting rod system



Fig. 2. Proposed connecting rod.

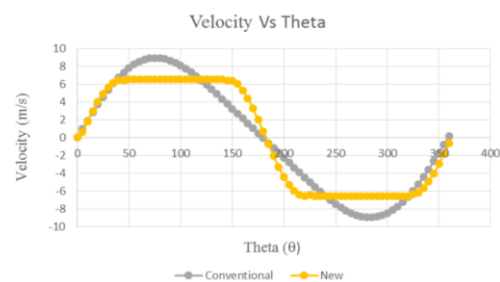


Fig. 3. Comparison of Velocity profile for Proposed and Conventional connecting rod system.

It is evident that, the mean value of velocity for the proposed connecting rod system is lesser than the conventional connecting rod system. The piston velocity for the conventional connecting rod arrangement seems to be continuously increasing till about 80° from TDC and then it is continuously decreasing for the remaining part of the stroke, which follows a Sinusoidal Curve Pattern. The maximum velocity reached about 9 m/s for conventional connecting rod system. On



Fig. 4. a Diesel Engine Experimental Setup.

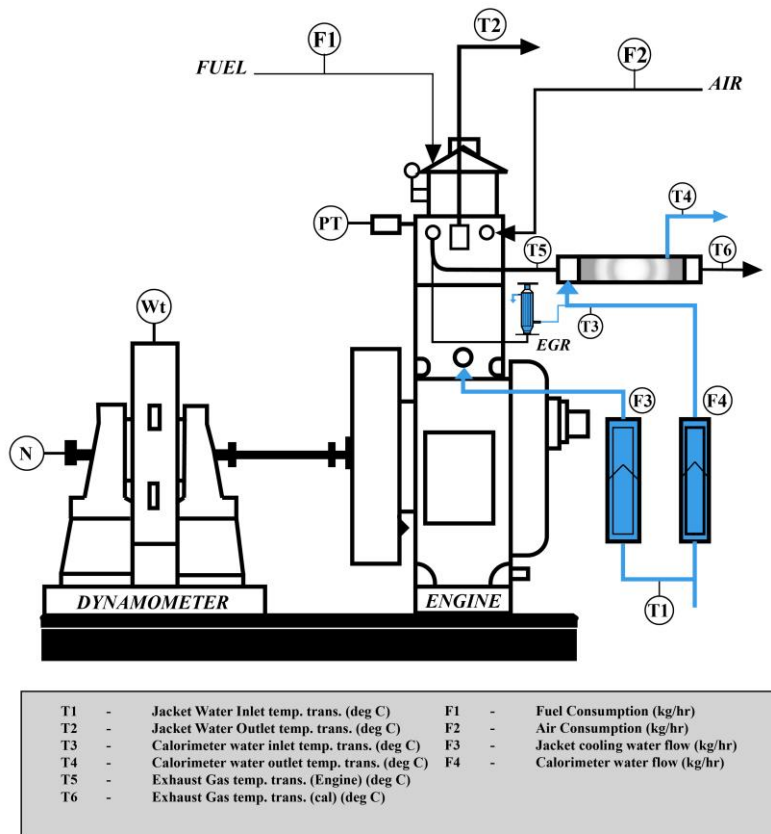


Fig – 4b Schematic Diagram of the Experimental Setup

comparison, behavior of the proposed connecting rod arrangement is found to be totally different. The piston velocity is increased till 6.6 m/s when the shaft rotation is about 40° from TDC and it remains uniform till the shaft rotates to 140°. The piston is moving at uniform velocity for next 100° of shaft rotation. This uniform piston movement also influences the rate of compression of the air in the cylinder during compression stroke. The Kinetic Energy possessed by the piston varies in a Trapezoidal manner with zero acceleration for

about 100° of shaft rotation.

3. EXPERIMENTAL PROCEDURE

Test were conducted on diesel engine by applying the load using hydraulic dynamometer. The pressure and various temperatures were measured for complete crank angle of every one degree variation. The output of the engine from analog to digital is analyzed by NI-DAQmx 8.6 software.

When the engine was running, the changes in the characteristics were observed and noted in personal computer. A mean value for 10 cycles were conducted and noted as a measurement specification for that load.

Test were conducted from no load condition to rated condition. In order to stabilize the engine at no load condition, engine was operated for 20 minutes. The engine was tested with diesel at various loads and the combustion and performance parameters were recorded. The experiments were conducted thrice to check the repeatability. The Diesel Engine experimental Setup and Schematic Diagram of the experimental Setup is shown in Fig. 4(a) and Fig. 4(b) respectively. The Diesel Engine Specifications is shown in Table 1.

4. CFD PROCEDURE

4.1. Meshing Methodology

Computational Fluid Dynamics methodology for the analysis of Compression-Ignition Engine involves with the physics that is highly transient, turbulent, includes with chemical reaction of different species, injection of diesel particles and finally involves with lot of moving parts. Surface clean-up, CFD domain extraction and surface meshing are done in ANSA. Different types of elements like tri, quad are appropriately used in defining non-conformal interfaces which facilitate motion of intake and exhaust valves. Geometrical Description of Combustion Chamber and Surface Discretization of different parts is shown in Fig. 5 and Fig. 6 respectively.

Table 1 Diesel Engine Specifications

Sl.No	Engine parameter	Specification
1	Make	Kirloskar
2	Cooling	Water
3	Bore × Stroke	87.5 × 110 mm
4	Compression Ratio	17.5:1
5	Cubic Capacity	661 cc
6	Rated Speed	1500 rpm
7	Number of Cylinders	One
8	Power	4.4 kW

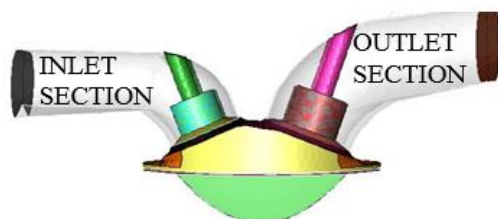


Fig. 5. Geometrical Description of Combustion Chamber.

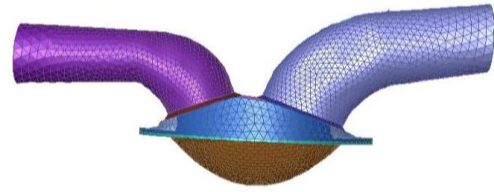


Fig. 6. Surface Discretization of different parts.

4.2. Dynamic Meshing and In-Cylinder Options

This work utilizes In-cylinder option of ANSYS Fluent to model the entire Internal Combustion Engine Cycle by providing crank shaft speed, connecting rod length, crank radius, crank period etc. (Jaya shankara *et al.*, 2010, Payri *et al.*, 2004). An in-built piston full, piston limit UDFs (User-defined functions) are used to model the piston motion and transient profiles to move the intake and exhaust valves.

To model the deforming zones three different strategies namely smoothing, dynamic layering and re-meshing methods are used in ANSYS Fluent. Smoothing and re-meshing algorithms are applied for tetrahedrons and layering uses hexahedron meshes. Smoothing algorithm adjusts the mesh with a moving and/or deforming boundary and the interior nodes without changing the number of nodes and their connectivity. For the large boundary re-meshing algorithm agglomerates cells that violate the skewness or size criteria and locally re-meshes the agglomerated cells or faces. In prismatic (hexahedral and/or wedge) mesh zones, dynamic layering can be used to add or remove layers of cells adjacent to a moving boundary, based on the height of the layer adjacent to the moving surface. Volume Discretization of different parts is shown in the Fig. 7.



Fig. 7. Volume Discretization of different parts.

4.3. Transport Equations for Fluid flow with Dynamic Zones

In general, for problems associated with Stationary Meshes Mass, Momentum and Energy Conservation laws are solved to find pressure P, three components of velocity u, v, w and temperature T.

The Non-Linear, Second Order, Non-Homogenous Equations are listed as

Conservation of Mass:

$$\frac{\partial \rho^*}{\partial t^*} + \rho^* \left[\frac{\partial u^*}{\partial x^*} + \frac{\partial v^*}{\partial y^*} + \frac{\partial w^*}{\partial z^*} \right] = 0 \quad (8)$$

Conservation of X Momentum:

$$\frac{\partial u^*}{\partial t^*} + (u^* \cdot \nabla^*) u^* = -\nabla^* p^* + \frac{1}{Re} \nabla^{*2} u^* + S_{Mx} \quad (9)$$

Where $u^* = u/U$

$v^* = v/V$

$w^* = w/W$

$\rho^* = \rho_{air}/\rho_{air@STP}$

$p^* = p/\rho U^2$

$t^* = t/t_{op}$ flow time in sec

$t_{op} = (L_c/U)$

t_{op} - Overall Period in sec, L_c - Characteristic length, U, V, W - Flow Velocity in x y and z directions respectively.

S_{Mx} - Source or Sink term for Momentum

Conservation of Energy:

Internal Energy:

$$\frac{\partial(\rho_i)}{\partial t} + div(\rho_i u) = -p div(u) + div(\mu grad T) + \Phi + S_i + S_{pi} \quad (10)$$

S_i - Source or Sink term for Energy

S_{pi} - Source or Sink term for Diesel Energy Particle

T - Temperature

Additional transport equations for turbulent properties such as k and epsilon are also solved for Re-Normalisation Group (RNG) k-Epsilon turbulence model. With moving boundaries and dynamic meshes the integral form of the conservation equation for a general scalar ϕ on an arbitrary control volume V whose boundary moving can be written as

$$\frac{d}{dx} \int_V \rho \phi dv + \int_{\partial v} \rho \phi (\vec{u} - \vec{u}_g) \cdot d\vec{A} = \int_{\partial v} \Gamma \nabla \phi \cdot d\vec{A} + \int_V S \phi dv \quad (11)$$

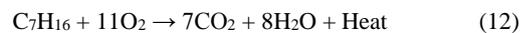
Where

\vec{u} is the Flow Velocity Vector, \vec{u}_g is the mesh velocity of the moving mesh, Γ is the Diffusion Coefficient, s_ϕ is the source term of ϕ , ϕ is any variable such as Pressure, Temperature etc.,

4.4. Combustion Modeling through Finite-rate Chemistry

The Combustion Modelling is done with Eddy Dissipation Model. Fuel burning inside the

combustion chamber is considered to be a single step finite rate chemical reaction (Qi *et al.*, 2011, Ge *et al.* 2009). Due to high temperature and high pressure inside the chamber after the compression stroke, the fuel automatically burns with some ignition-delay. The fuel burns quickly and the overall rate of reaction is controlled by turbulent mixing. The computational modelling of this combustion process is very expensive as well as time consuming. But the reaction rates can assumed to be controlled by the turbulence, ignoring the effect of chemistry timescales. Eddy Dissipation Model avoids expensive Arrhenius chemical kinetic calculations which is computationally cheap but produce realistic results (Dhuchakallaya *et al.*, 2010, Baker *et al.*, 1994). Diesel is assumed to n-heptane (C₇H₁₆) liquid and the corresponding stoichiometric balanced exothermic equation is



To model this species behaviour, a species transport equation in a convective-diffusive form is solved.

$$\frac{\partial}{\partial t} (\rho Y_i) + \nabla \cdot (\rho \vec{Y}_i) = -\nabla \cdot \vec{J}_i + R_i + S_i \quad (13)$$

Where Y_i is the Mass Fraction of each Species i , \vec{J}_i is the Diffusion Flux of Species i , R_i is the Net Rate of Production of Species i by Chemical Reaction, S_i - Source or Sink term for Energy.

4.5. Spray Modelling through Discrete Phase Model (DPM):

Addition of diesel particles inside the computational domain between particular crank angle intervals can be done using a lagrangian frame of reference. These diesel particles are dispersed into the continuous phase air and their coupling with continuous phase, combustion, break-up, coalescence, collision etc. can be calculated with discrete phase modelling.

The trajectory of a discrete phase particle is tracked by integrating the force balance equation on the particle that is written in a Lagrangian frame of reference. $\frac{\vec{u} - \vec{u}_p}{\tau_r}$ is the drag force per unit mass of the particle, \vec{F} indicates an additional acceleration term and $\frac{\vec{g}(\rho_p - \rho)}{\rho_p}$ is the body force.

$$\frac{d\vec{u}_p}{dx} = \frac{(\vec{u} - \vec{u}_p)}{\tau_r} + \frac{\vec{g}(\rho_p - \rho)}{\rho_p} + \vec{F} \quad (14)$$

τ_r is the relaxation time of the diesel droplet, \vec{u} is the velocity of the air, \vec{u}_p is the velocity of diesel droplet, μ is the viscosity, ρ is density of fluid, ρ_p is the density of diesel particle, d_p is the particle diameter and Re_c is the relative Reynolds Number.

The Relaxation Time and relative Reynolds

Number Equation is given as

$$\tau_r = \frac{\rho_p d_p^2 24}{18 \mu C_d R_e} \quad R_e = \frac{\rho d_p |\vec{u}_p - \vec{u}|}{\mu} \quad (15)$$

Different physics like heating and cooling, vaporization and boiling of diesel droplets are governed by certain laws and corresponding equations are solved. Secondary break up is modelled with wave model as the weber number exceeds more than 100 due to high velocity of diesel injection.

5. SOLVER METHODOLOGY

Flow is assumed to be three dimensional, unsteady and turbulent. Ideal Gas Law is used to model compressibility of air. Turbulence is modeled by EVM with RNG k-Epsilon model. RNG K-Epsilon model is a high Reynolds number model that solves two modified equations for K and Epsilon that has the ability to solve rapidly strained flows with high swirls. With effective meshing methodology, it can solve low Reynolds Number effects near the wall. Thus it is preferred over other models. PISO algorithm is used for pressure-velocity coupling. Second order approximation is used for flow, momentum and turbulent equations. DPM is used for particle tracking and EDM-Eddy Dissipation Model is used for modeling combustion.

5.1. Fluid and Boundary Conditions:

Air is assumed to be continuum fluid and Diesel particle is assumed to be discrete particle. Pressure inlet boundary condition is imposed at inlet boundary with 1 atmosphere (Total pressure). Pressure outlet boundary condition is imposed at outlet boundary with 1 atmosphere (Static pressure). Walls are assumed to be adiabatic with no slip condition. Piston Motion is controlled by User Defined Functions. Valve movements are included by transient profile.

6. VALIDATION STUDY

6.1. Grid Independence Study

Accuracy of numerical results strongly influenced by mesh size and mesh shape. With the increase in mesh count, accuracy of the numerical results increases considerably and also in the computational cost. One interesting feature about numerical approach is that there will be a point after which even if increase the mesh count considerably the accuracy of the results will not change too much. At this mesh count, the numerical results become independent of mesh count. To find this optimum mesh count, one needs to conduct a study called "Grid Independence Study". So that this mesh count can predict the results more accurately with minimum computational effort. In this work, Grid independent study is initiated with a mesh count around 0.1 million volume elements and

progressed randomly with increasing order. CFD results become almost closer with the experimental results. The difference between CFD and experimental results are around 7.0% at 0.4 million and after which the results are independent of mesh count. Details are shown in the Table 2 and Fig. 8. Thus, the volume mesh count around 0.4 million is considered for further studies.

6.2. Importance of Swirl, Tumble and Turbulence Intensity

Entire In-Cylinder physics is dominated by three essential flow parameters namely Turbulence Intensity, Swirl and Tumble (Prasad *et al.*, 2011, Mothilal *et al.* 2018). Swirl and Tumble enhances the acceleration of mixing of fuel and air where swirl promotes rapid combustion. Turbulence Intensity is the main measure that stabilizes the ignition process and higher its value assures faster propagation of flame. Squish is an additional flow parameter that exists for a short period during compression. In this work, these three properties are compared for the two different piston profiles over the entire cycle, particularly during intake and compression. Swirl Ratio and tumble ratio are two important measures that characterise the level of turbulence in the engine flow and the definition of these two parameters.

$$\text{Swirl Ratio } Sn = \frac{\omega_s}{2\pi N} \quad (16)$$

$$\text{Tumble Ratio } Tn = \frac{\omega_t}{2\pi N} \quad (17)$$

where ω_s and ω_t is the Angular Velocity of rotating flow at swirl axis and tumble axis respectively.

A custom field function is written in ANSYS-FLUENT for these two ratios as equations respectively and results are monitored for each crank angle.

$$\text{Swirl Ratio } Sn = \frac{L_s}{I_s} / \frac{2\pi N}{60} \quad (18)$$

$$\text{Tumble Ratio } Tn = \frac{L_t}{I_t} / \frac{2\pi N}{60} \quad (19)$$

Where L_s and L_t are the angular momentum with respect to swirl and tumble axis respectively, I_s and I_t are the moment of inertia with respect to swirl and tumble axis respectively.

7. PERFORMANCE COMPARISON OF SINUSOIDAL AND TRAPEZOIDAL PROFILE

Four different Trapezoidal Profiles are established and the flow and thermal behaviour of each one is tested using CFD. The optimum Trapezoidal Profile is selected in such a way that the hydrodynamic behaviour (Senthil Kumar *et al.* 2010) remains so

Table 2 Mesh Count Deviation between Experimental and CFD Results

Mesh Count	Difference between Experimental and CFD Results (%)
96,730	12.4
1,42,124	9.65
2,11,875	8.82
3,08,976	7.15
3,96,525	6.98
4,70,744	6.80

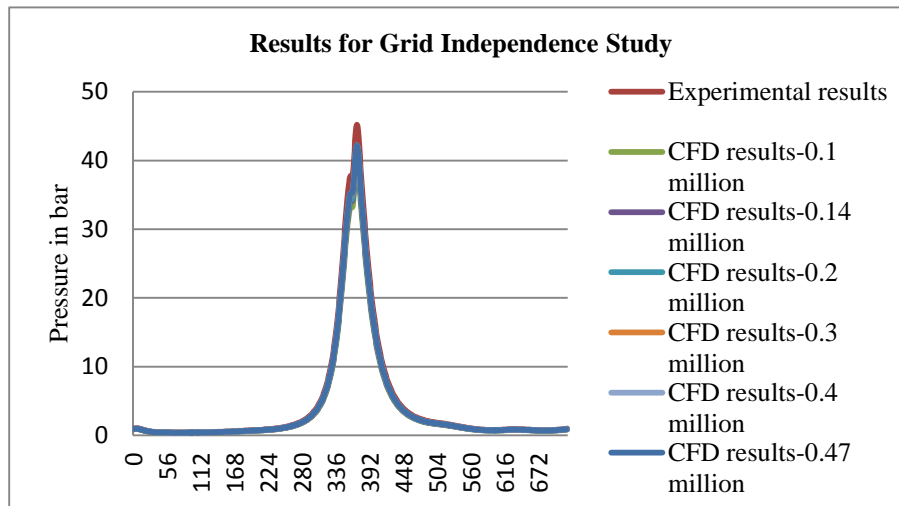


Fig. 8. Pressure –Crank Angle (θ).

close to Sinusoidal Profile but with reduced velocity.

From the plots and graphs for Sinusoidal and optimum Trapezoidal Piston Profiles, it is found that minimum variation in the flow pattern and level of Turbulence Intensity. This minimum variation of flow pattern and level of Turbulence Intensity prevails for most of the crank angle such that the internal flow behaviour, turbulence characteristics, swirl and tumble ratios remain almost similar for existing Sinusoidal Movement.

CFD results at different crank angle:

At 60° crank angle (During intake stroke):

From the velocity plots at 60° crank angle, the velocity distribution of air remains almost the same with average velocity which is around 48 m/s. Velocity vector indicates the presence of a swirl that occurs in virtually similar location in both combustion chamber. In spite of having substantial variation in the Turbulence Intensity (TI) pattern, values are closer for both cases which is shown in Fig. 9.

At 180° crank angle (End of intake stroke):

At this crank angle, an extended swirl is seen at the chamber which has higher magnitude of velocity in case of Sinusoidal Profile comparing to Trapezoidal Profile. TI and velocity vectors shows variation

two different configurations. This ensures that the power and thermal characteristics are almost analogous for both profiles with considerable reduction of friction losses in the Trapezoidal Profile. Around 10% friction loss and 7% pumping losses are reduced in optimum Trapezoidal Trajectory with substantial reduction of inertia force on the mechanical system and noise due to vibration. Thus it can be concluded that the optimum Trapezoidal Trajectory for the piston movement is comparably more efficient than the between these two profiles though the values remain nearer which is shown in Fig. 10.

At 350° crank angle (during compression stroke-before ignition):

The degree of closeness of results are negligible during compression that can be seen from the results for this case. Values and distribution of most of the flow variables are significantly close at this angle which is shown in Fig. 11.

The Swirl and Tumble Ratio Plots:

The Swirl and Tumble Ratio values are plotted for every crank angle till 180° which is shown in Fig. 12 and Fig. 13 respectively. Comparing to Trapezoidal Profiles for other modules that are experimented, this case with 26 teeth in internal gear and 18 teeth in pinion is found to have substantial intimacy with Sinusoidal Profile.

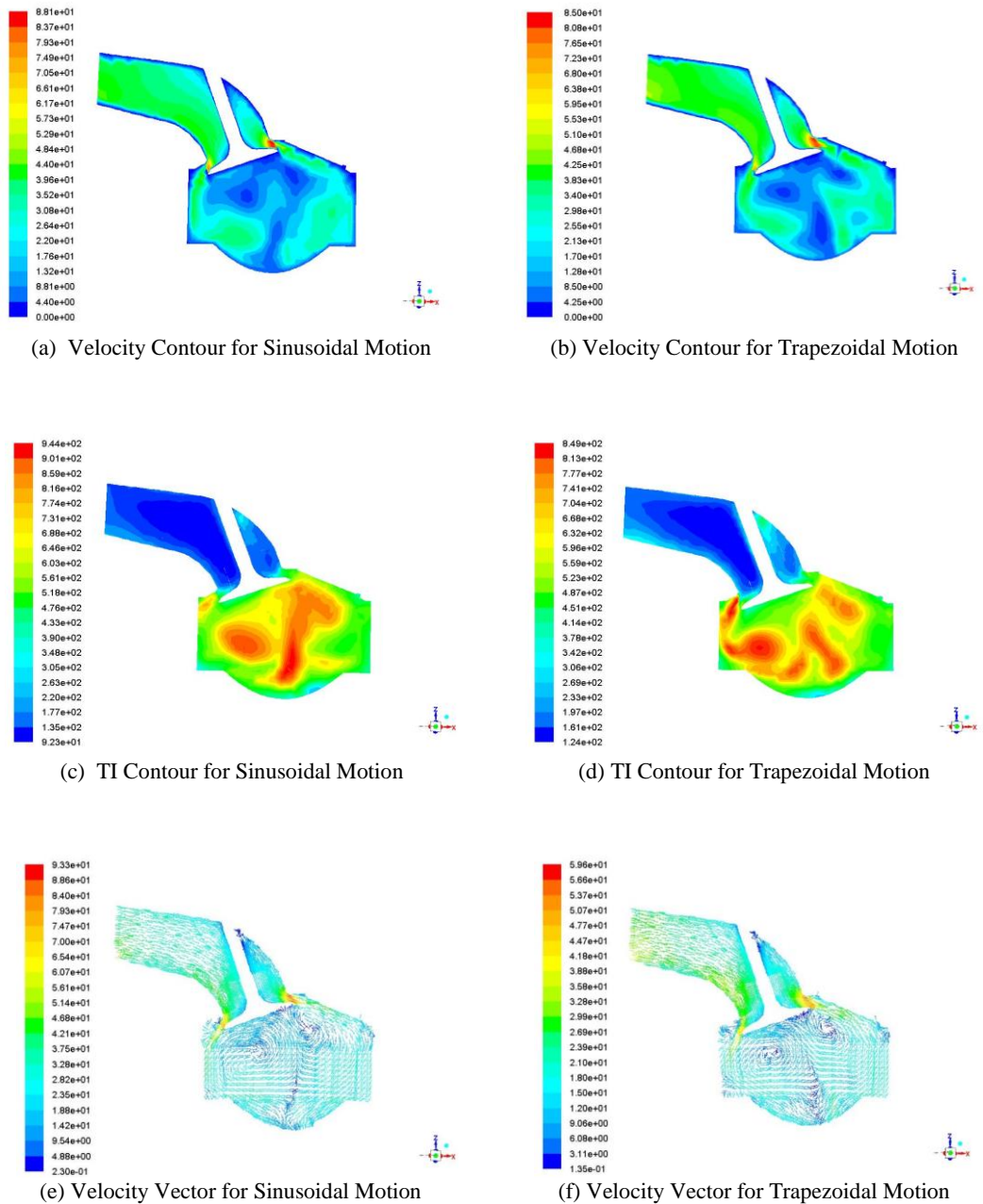


Fig. 9. Velocity Contour, TI Contour and Velocity Vector for Sinusoidal Motion and Trapezoidal Motion at 60° crank angle.

8. CONCLUSION

A notable effort is attempted to understand the problems associated with existing Sinusoidal Piston Trajectory. The continuous accelerating and retarding Sinusoidal Piston Profile generates frictional losses, jerk and finally noise. To overcome these drawbacks, an alternative Trapezoidal Piston Trajectory that has constant velocity is proposed. The less mean velocity and smooth transition of this profile for most of the crank angle contributes improved performance. A

special connecting rod is devised with an internal gear and pinion arrangement. With different pinion and gear teeth combination many Trapezoidal Profiles are arrived. To compare these profiles CFD is chosen due to the complexities of experimental investigation. The optimum Trapezoidal Profile is identified, that has significant similarity with Sinusoidal Piston in terms of flow, thermal and turbulent characteristics but with considerable reduction of mean velocity. This, in turn, reduces various losses like pumping and friction by almost 10% and increase the efficiency of the engine.

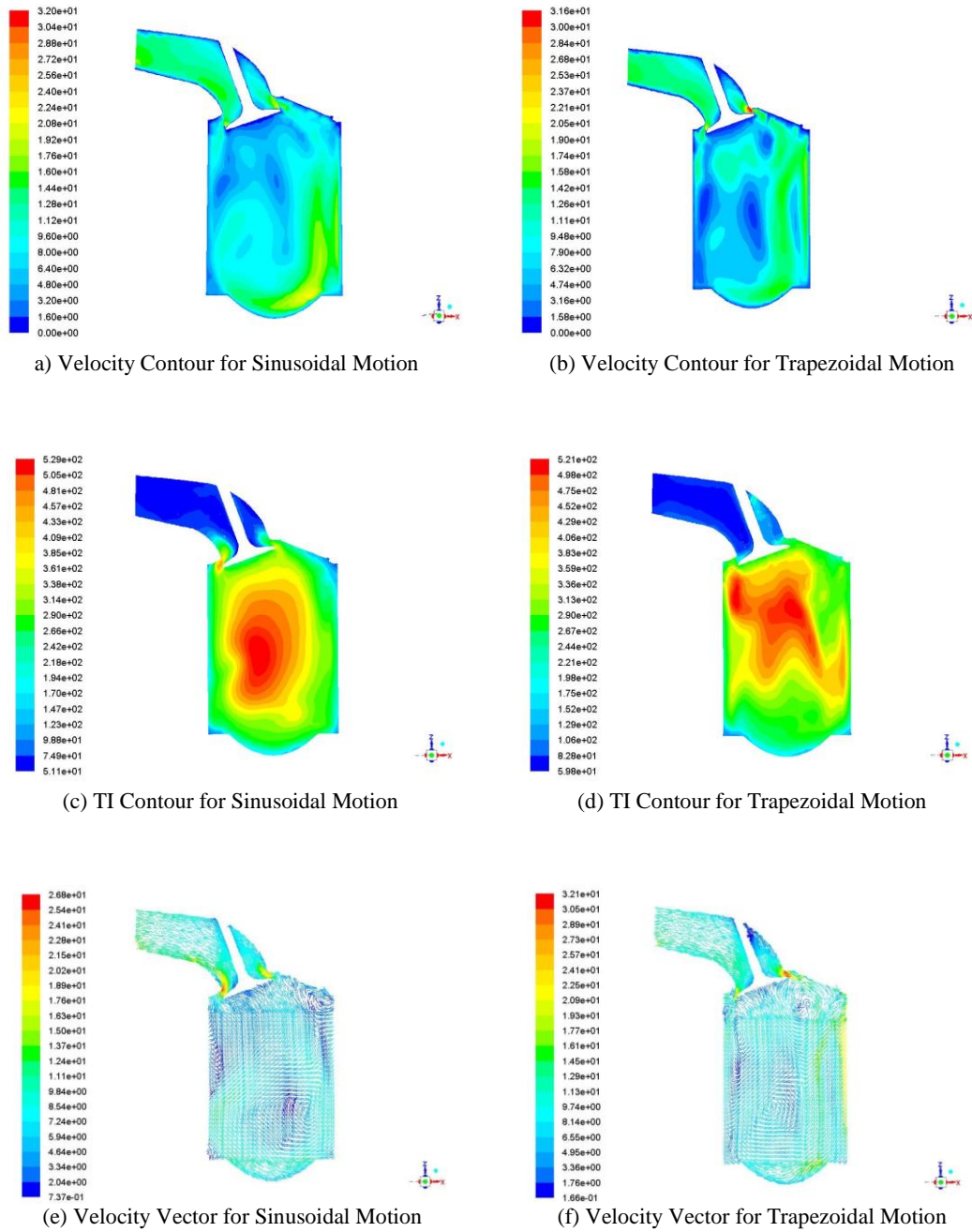


Fig. 10. Velocity Contour, TI Contour and Velocity Vector for Sinusoidal Motion and Trapezoidal Motion at 180° crank angle.

ACKNOWLEDGEMENTS

The authors wish to extend their gratitude to the SRM Eswari Engineering College, Chennai and Velammal Institute of Technology, Chennai for their tremendous and continuous support to carry out this research work.

REFERENCES

Badescu, V. (2004). Optimal paths for minimizing

lost available work during usual heat transfer processes. *Journal of Non-Equilibrium Thermodynamics* 29 (1) 53-73.

Baker, D. M. and D. N. Assanis (1994). A Methodology for coupled thermodynamic and heat transfer analysis of a diesel engine. *Applied Mathematical modelling* 18(11), 590-601.

Chen, L., S. Xia and F. Sun (2009). Optimal paths for minimizing entropy generation during heat transfer processes with a generalized heat

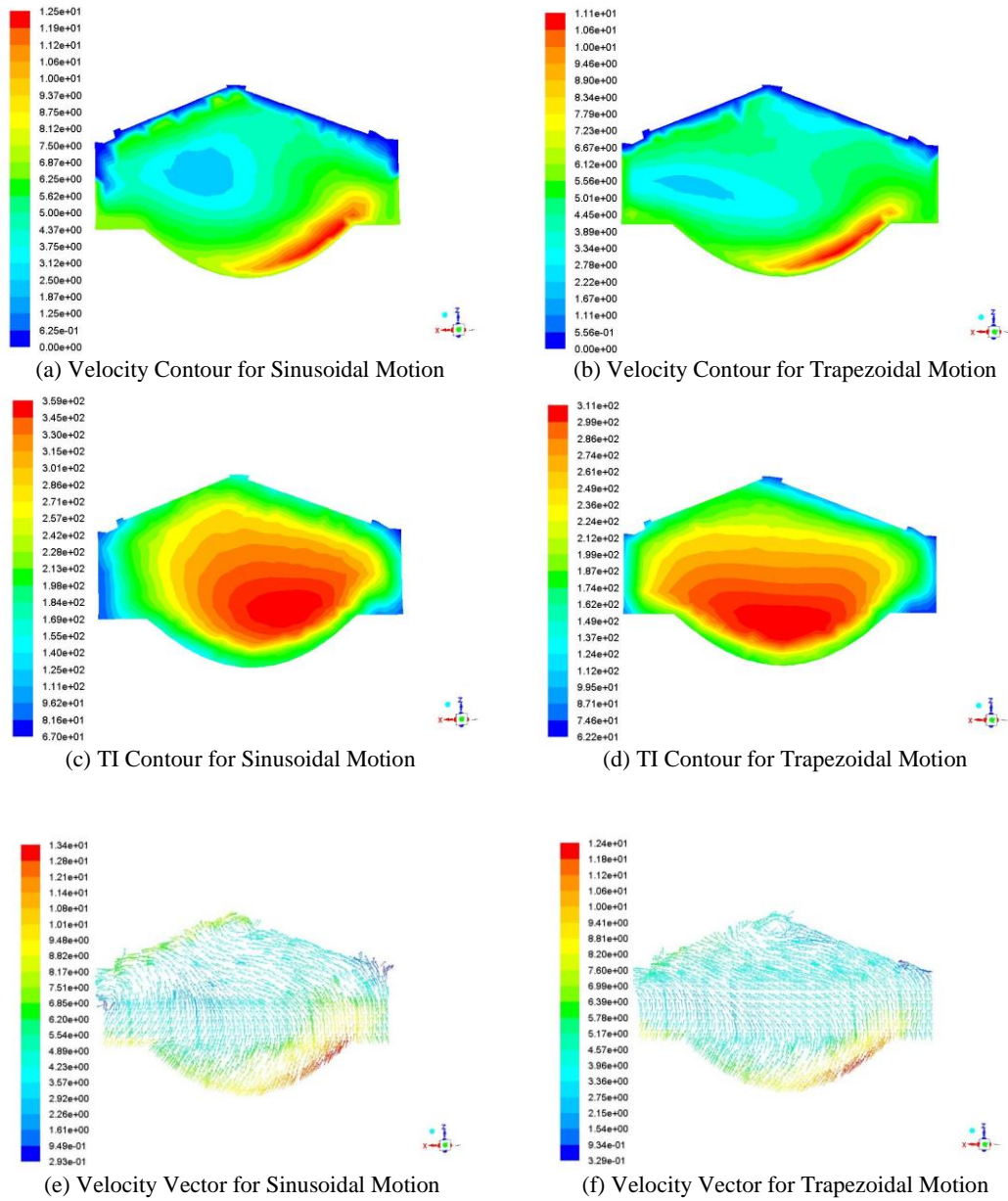


Fig. 11. Velocity Contour, TI Contour and Velocity Vector for Sinusoidal Motion & Trapezoidal Motion at 350° crank angle.

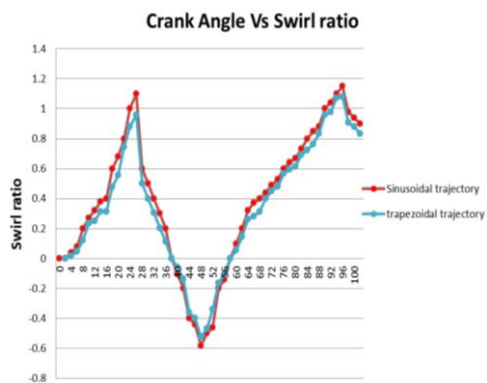


Fig. 12. Crank Angle Vs Swirl Ratio.

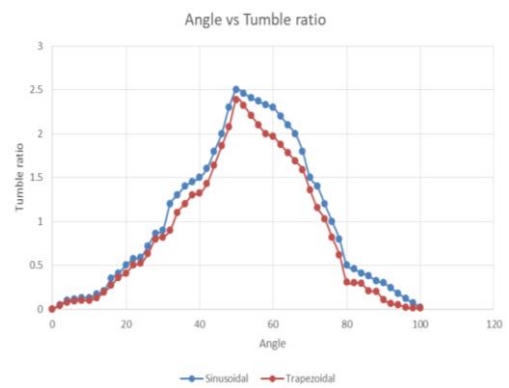


Fig. 13. Crank Angle Vs Tumble Ratio.

- transfer law. *Journal of Applied Physics* 105, 044907-1-5.
- Chen, L., S. Xia and F. Sun (2011). Optimizing piston velocity profile for maximum work output from a generalized radiative law Diesel engine. *Mathematical and Computer Modelling* 54, 2051-2063.
- De Vos, A. (1985). Efficiency of some heat engines at maximum power conditions. *American Journal of Physics* 53(6), 570-573.
- Dhuchakallaya, I. and A. P. Watkins (2010). Auto-ignition of diesel spray using the PDF-Eddy Break-Up model. *Applied Mathematical Modelling* 34(7), 1732-1745.
- Ge, Y. L. Chen and F. Sun (2009). Finite-time thermodynamic modeling and analysis for an irreversible Dual cycle. *Mathematical and Computer Modelling* 50 (1/2), 101-108.
- Jaya shankara, B. and V. Ganesan (2010). Effect of fuel injection timing and intake pressure on the performance of a DI diesel engine-A parametric study using CFD. *Energy conversation and management* 51, 1835-1848.
- Kamil, M., M. M. Rahman and R. A. Bakar (2014). An Integrated Model for Predicting Engine Friction Losses in Internal Combustion Engines. *International Journal of Automotive and Mechanical Engineering* 9, 1695-1708.
- Mothilal, T., K. Pitchandi, V. Velukumar and K. Parthiban (2018). CFD and Statistical Approach for Optimization of Operating Parameters in a Tangential Cyclone Heat Exchanger. *Journal of Applied Fluid Mechanics* 11(2), 459-466.
- Nigus, H. (2015). Kinematics and Load Formulation of Engine Crank Mechanism. *Mechanics, Materials Science & Engineering* 1,112-123.
- Payri, F., J. Benajes, X. Margot and A. Gil (2004). CFD modeling of the in-cylinder flow in direct injection diesel engines. *Computer & Fluids* 33, 995-1021.
- Prasad, B. V. V. S. U., C. S. Sharma, T. N. C. Anand and R. V. Ravikrishna (2011). High swirl-inducing piston bowls in small diesel engines for emission reduction. *Applied Energy* 88, 2355–2367.
- Qi, K., L. Feng, X. Leng, B. Du and W. Long (2011). Simulation of quasi-dimensional combustion model for predicting diesel engine performance. *Applied Mathematical modelling* 35(2), 930-940.
- Rakopoulos, C. D., G. M. Kosmadakis and E. G. Pariotis (2010). Investigation of piston bowl geometry and speed effects in a motored HSDI diesel engine using a CFD against a quasi-dimensional model. *Energy Conversion and Management* 51, 470–484.
- Rubin, M. H. (1979). Optimal configuration of a class of irreversible heat engines. II. *Physical Review A* 19, 1277-1289.
- Senthil Kumar, M, M, P.R.Thyla and E. Anbarasu (2010). Numerical analysis of hydrodynamic journal bearing under transient dynamic conditions. *Mechanika. - Kaunas Univ Technology* 2(82), 37-42.
- Shyy, W. (1994). *Computational modeling for fluid flow and interfacial transport* 1st Edition, Elsevier Science.
- Taylor, C. F. (1966). *The Internal Combustion Engine in Theory and Practice* (MIT Press, Cambridge, MA) 1, 158-164, 2, 19-20.
- Teh, K. Y. and C. F. Edwards (2006). An Optimal Control Approach to Minimizing Entropy Generation in an Adiabatic IC Engine with Fixed Compression Ratio. in: *Proceedings of IMECE2006, IMECE2006-13581, 2006 ASME International Mechanical Engineering Congress and Exposition, Chicago, Illinois, USA.*
- Teh, K. Y. and C. F. Edwards (2006). Optimizing piston velocity profile for maximum work output from an IC engine, in: *Proceedings of IMECE2006, IMECE2006-13622, 2006 ASME International Mechanical Engineering Congress and Exposition, Chicago, Illinois, USA.*